Sticker-Type Hybrid Photoplethysmogram Monitoring System Integrating CMOS IC With Organic Optical Sensors

Yongsu Lee, *Member, IEEE*, Hyeonwoo Lee, Jaeeun Jang, Jihee Lee, Minseo Kim, Jaehyuk Lee, Hyunki Kim, *Student Member, IEEE*, Seunghyup Yoo, *Member, IEEE*, and Hoi-Jun Yoo, *Fellow, IEEE*

***Abstract*— A sticker-type system with hybrid integration of CMOS IC and organic optical sensors is proposed to monitor photoplethysmogram (PPG) signals. To solve problems with the previous solely organic sensor-based works, CMOS IC is implemented in 180 nm technology under 5 V/1.5 V dual power supply. The silver-wire printed planar-fashionable circuit board (P-FCB) is used to connect the CMOS IC with organic sensors. The proposed hybrid system has the five following key features: 1) Power-efficient structure of organic sensor; 2) Integrated analog front-end and digital processor; 3) Degradation compensation scheme; 4) Large parasitic elements optimized design; and 5) Motion artifact rejection scheme. The sticker-type PPG monitoring system has mass of only 2g, including the batteries, and consumes only 233 μW to operate. The PPG signal could be acquired from various body parts (finger, wrist, and neck). The peripheral oxygen saturation level (SpO_2) extraction results are verified by comparison with a commercial sensor device.**

***Index Terms*— CMOS IC, hybrid integration, low-power, motion artifact rejection, organic optical sensor, photoplethysmogram (PPG), sticker-type system.**

I. Introduction

A PHOTOPLETHYSMOGRAM (PPG) is an optically obtained biomedical signal containing data on the volumetric change of arteries and arterioles in the subcutaneous tissue [1]. The PPG signal is easy to measure, and it can be used to diagnose various medical symptoms. Fig. 1 shows the applications of the PPG signal measurement. The heart rate variation (HRV) can be attained from the time difference between peaks of the PPG signal. HRV extraction from the PPG signal can be performed on just a single spot of the human body, whereas the electrocardiogram (ECG) based method needs measurements from multiple body parts [2]. In addition, a peripheral oxygen saturation level (SpO_2) can be extracted from two different wavelengths of the PPG signals [3]. The ratio of AC and DC components of the PPG signals are used to calculate the value of SpO_2.

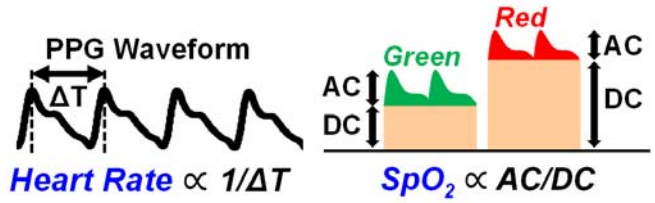

Fig. 1. Medial Indicators Extracted from the PPG Signal.

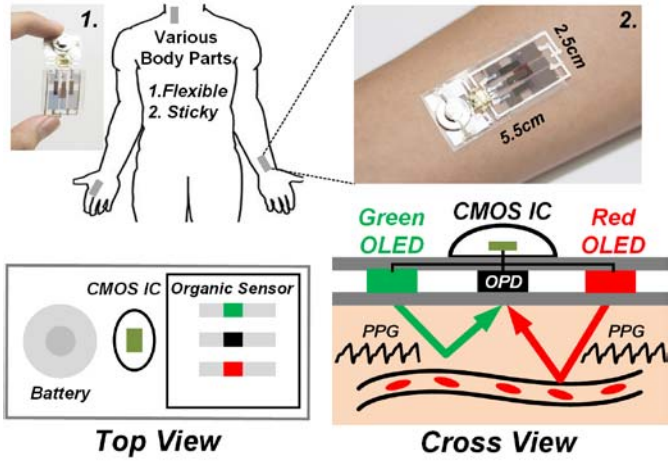

Fig. 2. PPG Signal Acquisition with Sticker-type Hybrid System.

SpO_2 is one of the most important vital signals for patients in the intensive care unit. It reflects the health of the cardiopulmonary system [4]. Recently, organic optical sensor-based PPG signal acquisition systems were reported [5]-[7]. In particular, a sticker-type sensor system was proposed for user convenience [7]. The previous, solely organic sensor-based systems have several problems when utilized for daily PPG signal monitoring, in terms of practicality [5]-[6].

In this paper, a hybrid integration of CMOS IC with organic optical sensors is proposed to solve the problems of previous systems. As shown in Fig. 2, a sticker-type sensor system

Manuscript received May 30, 2016; revised August 12, 2016; accepted September 27, 2016. This paper was approved by Guest Editor Eduard Alarcon. This work was supported by the Open Innovation Lab Project from National Nanofab Center (NNFC). This paper was recommended by Guest Editor J. S. Chang

The authors are with the School of Electrical Engineering, Korea Advanced Institute of Science and Technology (KAIST), Daejeon 305-701, Republic of Korea (e-mail: yongsu@kaist.ac.kr).

Color versions of one or more of the figures in this paper are available online at http://ieeexplore.ieee.org.

Digital Object Identifier 10.1109/JETCAS.2016.2630301

is proposed for PPG signal acquisition with the reflective method. The small system (5.5 × 2.5 cm) can be attached to various body parts (neck, wrist, and fingertip) due to its flexible body and adhesive backside. As shown in the top view of the system, the CMOS IC is integrated with organic optical sensors. A green and a red organic light-emitting diode (OLED) are used for the light emitting elements and an organic photodiode (OPD) between the two OLEDs is implemented as the light receiving element, as shown in the cross view. The integrated CMOS IC controls the organic optical sensors with analog front-end and the measured PPG data is collected and processed with the internal digital processor. Furthermore, the proposed CMOS IC has a motion artifact rejection scheme for more stable acquisition of the PPG signal.

This paper is organized as follows. In section II, the problems of previous organic sensor based PPG acquisition systems are described. In section III, the features and advantages of the proposed hybrid system are shown. In section IV, the method used to connect the CMOS IC and the organic optical sensors is explained. Implementation and measurement results of the proposed system are shown in section V. Section VI contains the conclusions.

II. Limitations of Previous "Organic-Based" PPG Signal Acquisition Systems and Other Practical Considerations

A. Form-Factors and Power Efficiency

Recent work by Claire et al. successfully demonstrated the feasibility of using organic devices for the sensing element of PPG acquisition system [5]. However, it was made as a transmitted type on rigid glass substrates; to better utilize the merits of organic sensors, a patch or sticker-type sensor system is more suitable for seamless integration on to a human body. To this end, the proposed system uses flexible substrate and acquires the PPG data from body-reflected light to form a sticker-type sensor system. As mentioned in section I, two different wavelengths of PPG signals are required to extract the SpO_2 value. Due to the characteristic that optical reflectivity gets higher at shorter wavelengths [8], the wavelength of the green band (510 - 530 nm) is better than the infra-red band (900 - 1000 nm) in terms of low-power consumption for patch or sticker-type PPG acquisition systems, as shown in Fig. 3.

In addition, power inefficient, polymer-based light emitting diodes (PLEDs) were adopted as light sources in previous works [5]-[6]. The power efficiencies of the previous PLEDs [9]-[12] varied from 1 to 29 lm/W, making them less suitable for 24/7 continuous PPG monitoring systems.

B. Absence of Integrated Analog Front-end and Digital Processor

The following two elements are needed to measure a PPG signal accurately: analog front-end and digital processor. The analog front-end applies proper current to the OLED to emit light and senses the current generated from the OPD using light reflected from the body. The digital processor controls the overall system and collects digital-converted PPG data.

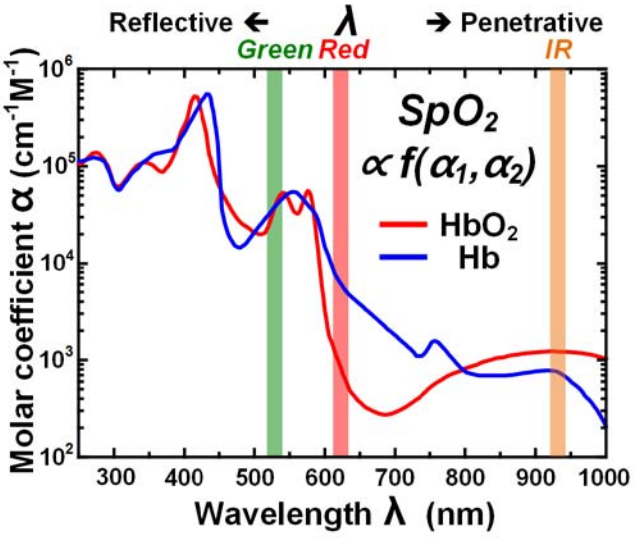

Fig. 3. Light Wavelength Band Selection for SpO_2 Extraction.

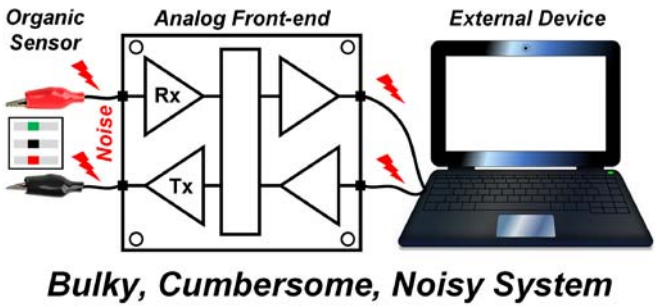

Fig. 4. Problems Due to Absence of Integrated Analog Front-end & Digital Processor.

In previous solely organic sensor based PPG acquisition systems [5]-[6], the analog front-end and digital processor were composed of bulky and cumbersome external components like crocodile clips or commercial off-the-shelf-connectors (Fig. 4). Those systems are not so suitable for wearable devices, and continuous monitoring is very hard to maintain in terms of small form-factor. Furthermore, the long cables connecting the sensors and analog front-end largely degraded the acquired signal-to-noise ratio (SNR). Previous active electrode (AE) systems were proposed for enhancing signal quality [13]-[14]. The CMOS IC is an essential requirement for a compact and low-noise PPG acquisition system.

C. Degradation of Organic Sensor

Every organic sensor suffers from performance degradation with the passage of time [15]. The luminance of an OLED with the same current and responsivity of the OPD tends to decrease due to the chemical reaction of the organic devices with the oxygen and moisture in the atmosphere. In some cases, dark spots emerge on the surface of organic sensors causing large deterioration of performance. Fig. 5(a) shows the principle of how a dark spot is generated in the organic sensors [16].

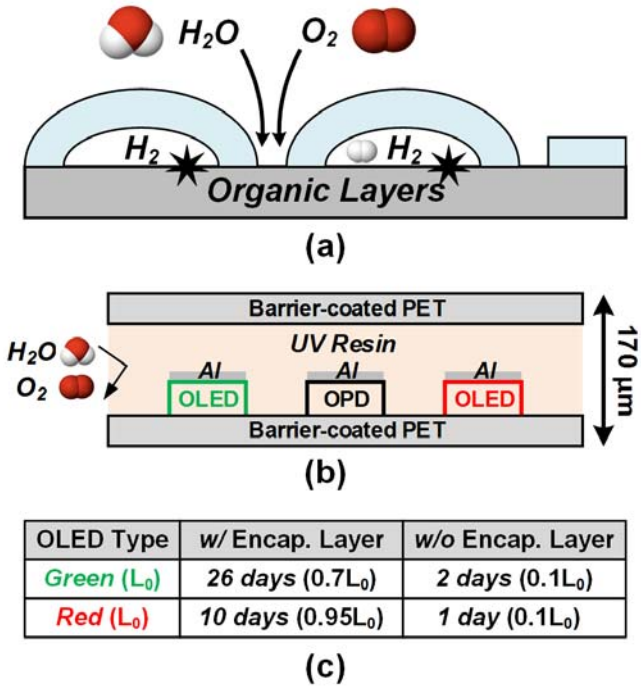

OLED Type	*w/* Encap. Layer	*w/o* Encap. Layer
Green (L_0)	*26 days* ($0.7L_0$)	*2 days* ($0.1L_0$)
Red (L_0)	*10 days* ($0.95L_0$)	*1 day* ($0.1L_0$)

(c)

Fig. 5. (a) Principle of Degradation (b) Face-Seal Encapsulation Scheme Adopted in This Work (c) Degradation of OLEDs with and without Encapsulation Structure

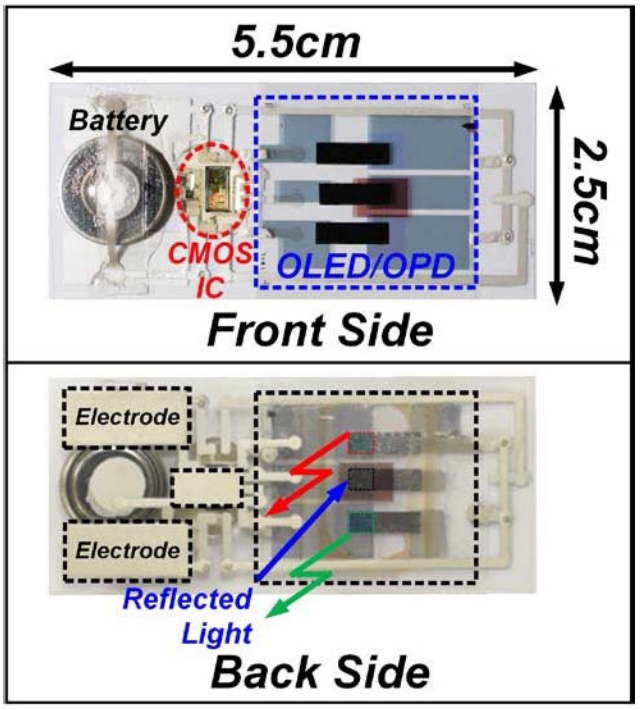

Fig. 6. Proposed Sticker-typed Hybrid System Configuration

The hydrogen (H_2) bubbles are created from the chain chemical reaction of oxygen and moisture with the organic compounds or with electrode materials. In order to prevent this degradation phenomenon, an encapsulation layer is coated on top of the organic sensor. Fig. 5(b) shows an example of encapsulation scheme, called 'face-seal encapsulation,' which is known to be effective in protecting flexible organic devices from moisture and oxygen [17]. Fig. 5(c) shows the luminance reduction results of the proposed OLED as time passes. Without the encapsulation layer, the luminance is dramatically reduced to one-tenth of original value just in a day. On the other hand, 70% of the luminance is maintained even after a month with the protection of the encapsulation layer. In spite of the encapsulation layer, an additional performance compensation scheme is needed to achieve an accurate, continuous PPG signal monitoring system.

D. Large Parasitic Elements of Organic Sensors

The OLED and OPD have large parasitic elements, especially parasitic capacitance. This is, because they are composed of large-area-occupying high-permittivity organic components [18]. The large parasitic elements put restrictions on fast frequency operation of organic sensors. Therefore, duty-controlled current applying or current sensing for low-power consumption can be limited by the value of the parasitic elements of the organic sensors. Furthermore, the large parasitic capacitance can influence the noise characteristics of the current sensing systems [19]. Therefore, a well-designed analog front-end for large capacitance of OPD is required to meet minimum requirements for PPG SNR.

E. Motion Artifact

The motion artifact is a very important consideration for wearable monitoring systems [20]. The motion artifact makes the DC value of measured signal fluctuate. As a result, motion artifact largely affects the PPG monitoring system because the ratio of the AC and DC components of a PPG signal is very low (0.005 - 0.1). Therefore, a motion artifact rejection scheme is required for a wearable PPG signal monitoring system.

III. Design of the Proposed Hybrid System

The special functionality of the CMOS IC enables the use of a sticker-type hybrid integration system that solves the five abovementioned problems. Fig. 6 shows the configuration of the proposed hybrid system. The sticker-type system is 5.5 cm $\times$ 2.5 cm. On the front side of the system, coin-cell batteries are integrated to supply power. Next to the battery, the CMOS IC is integrated, and the OLEDs and OPD are implemented beside the CMOS IC. Every component is connected with the others by a screen printed silver wire called planar-fashionable circuit board (P-FCB) technology [21]. On the back side of the system, the green and red band of OLEDs illuminates toward the body and the OPD senses reflected light. The two silver electrodes printed on the back side of the system are for monitoring contact impedance. The small electrode in the center is used as the reference voltage electrode. The advantages of the proposed hybrid system, and methods used for solving the five problems, are introduced in the following sections.

A. Power-efficient Structure of the Organic Sensor and Flexible Form-factor

As mentioned in section II-A, power-inefficient PLEDs were adopted as the light sources in previous PPG monitoring

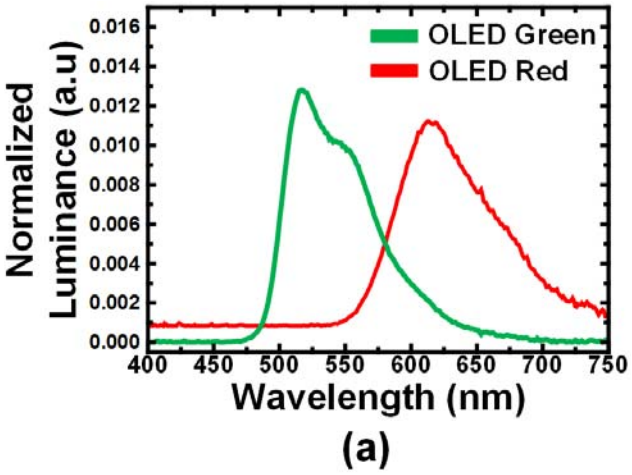

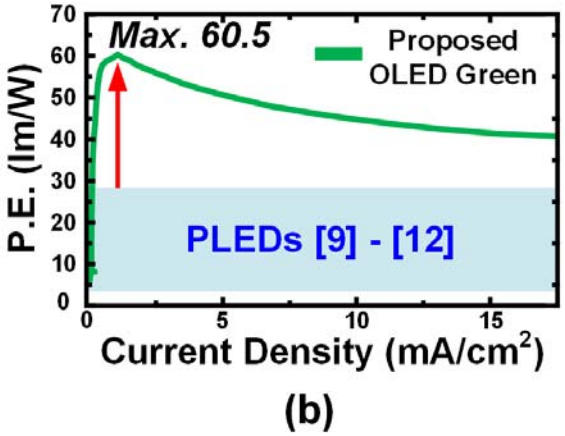

Fig. 7. Specifications of Green & Red OLED (a) Normalized Luminance According to Wavelength, (b) Power Efficiency of Proposed Green OLED.

systems [5]-[6]. In the proposed work, the OLEDs are composed of power-efficient low-molecular weight organic elements. The top electrode is manufactured with LiF/Al, and polyethylene terephthalate (PET) film is used as the bottom substrate layer. Transparent IZO is used as the bottom electrode, because the OLED emits light downward. In addition, IZO has high conductivity (40–80 Ω/square) and can be manufactured with a low-temperature process so that it can be prepared on flexible substrates. The total thickness is only 350 nm for the green OLED and 360 nm for the red OLED. The normalized luminance spectra of the OLEDs are shown in Fig. 7(a). The 520 and 610-nm centered green and red bands are adopted as the light sources for PPG signal acquisition. In the previous PLED-based works [9]-[12], the maximum reported power efficiency was 28.54 lm/W. Meanwhile, the maximum power efficiency of the proposed green OLED is 60.5 lm/W as shown in Fig. 7(b).

The top electrode of OPD is thermally evaporated Al. PET film is used as the bottom substrate layer (shared with the OLEDs). The transparent IZO is used as the bottom electrode, because the OPD senses the light reflected from the body from below. A layer of C_{70} doped with 4, 4′-Cyclohexylidenebis [N,N-bis(4-methylphenyl)benzenamine] (TAPC) is used for high responsivity [22]. A low dark-current value (10^{-10}A) with 0 V bias is achieved by optimizing the hole-transport layer. The responsivity of the OPD according to wavelength is shown in Fig. 8. The proposed OPD can achieve enough responsivity (>0.2 A/W) in the target green and red bands.

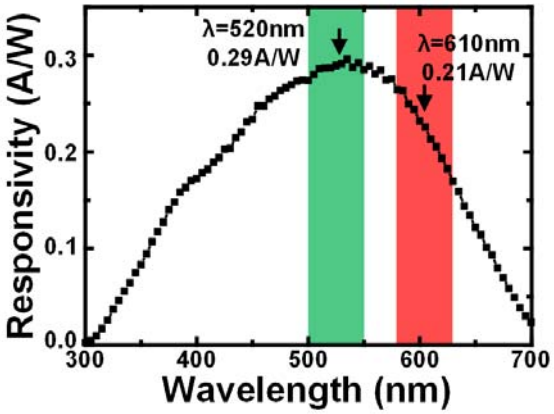

Fig. 8. Specifications of OPD: Responsivity According to Wavelength.

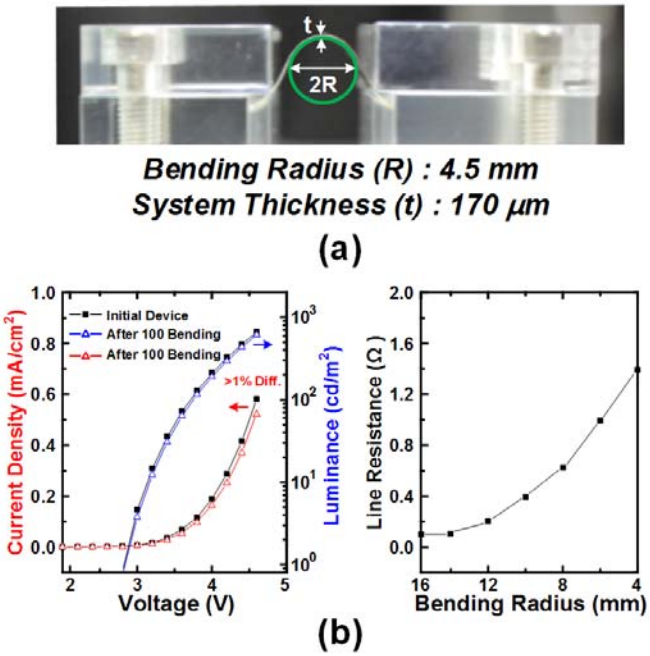

Fig. 9. (a) Custom-made Setup for Flexibility Test, (b) Optical and Electrical Property Change with Bending: Characteristics of OLEDs (Left) and Line Resistance of Silver Wire (Right).

Being fabricated on a PET substrate, the proposed organic devices are mechanically flexible. Fig. 9 (a) and (b) how that the device performance can hold well even after 100-time bending (tensile stress) at the bending radius of 4.5 mm, which is small enough to use on a part of human body typically adopted for PPG acquisition. Less than 1% luminance change occurred after repeated bending, for instance. The line resistance of the silver wire is shown to increase after being bent at such a small bending radius, but it is still small (1.5 Ω) enough to operate the system. Furthermore, use of a thin substrate makes the organic sensor less sensitive to ambient

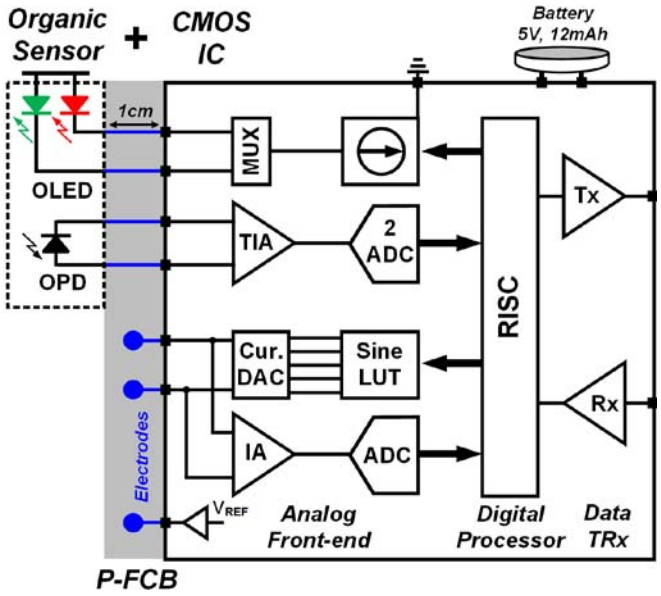

Fig. 10. Overall Architecture of the Hybrid System.

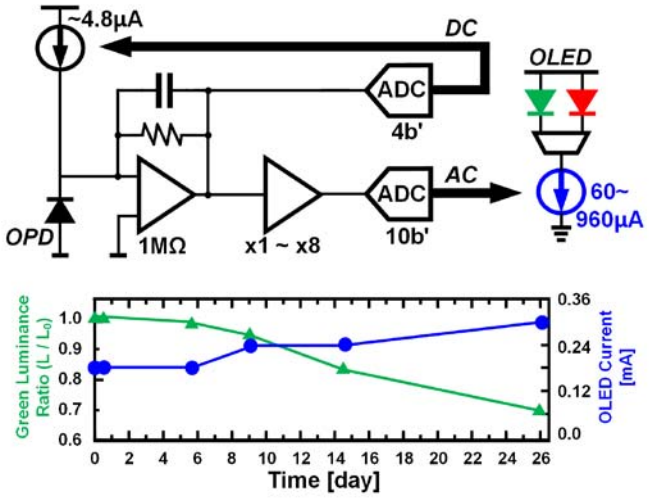

Fig. 11. Organic Optical Sensor Degradation Compensation with CMOS IC.

light interference, which may further be suppressed, if needed, easily by blocking the top part of the sensor part with any black materials.

B. Integrated Analog Front-end and Digital Processor

In the proposed system, CMOS IC is hybrid integrated with the organic optical sensors to achieve a small form-factor and low-noise system. The CMOS IC and light diodes are integrated on a small piece (5.5 × 2.5 cm) of PET film, and each component is connected using P-FCB silver wires. The distance between organic sensors and CMOS IC is <1 cm. Fig. 10 shows the overall architecture of the hybrid system. The CMOS IC is composed of the analog front-end, internal digital processor, and data transceivers. For lighting the OLEDs, current steering DACs of the analog front-end are used for the adaptive current supply. The amount of current flow is determined by the digital processor. The detailed process will be explained in section III-C. The OPD responds to the body-reflected light, and current generated from the OPD is amplified with the trans-impedance amplifier (TIA) of the analog front-end. The gain of the TIA is 1 MΩ, and variable gain (1–8) is adaptively applied in the 2nd amplifier. The acquired PPG data is sampled with two types of ADCs – 4b′DC sampled SAR ADC, and 10b′AC sampled SAR ADC. The sampled data is stored in the internal memory of the digital processor. For motion artifact rejection, contact impedance data is measured. The pseudo-sine wave current is generated in the analog-front end and used to stimulate the body. The contact impedance is measured with the low-noise amplifier (LNA) of the analog front-end, and the analog data is converted to digital values via 10′b SAR ADC. The sampled contact impedance data is collected by the digital processor, and used for the motion artifact rejection scheme. The detailed process will be explained in section III-E. The received and refined PPG data is then transferred to an external data-hub, such as a smart device or hospital server, through data transceivers.

C. Degradation Compensation Scheme

As mentioned in section II-C, the performance degradation of organic optical sensor should be compensated in spite of the encapsulation layer. Fig. 11 shows the degradation compensation scheme of the proposed hybrid system. At first, the PPG signal from the OPD is measured with gain-of-1-MΩ TIA in the CMOS IC. The DC value sampled with the 4′b SAR ADC decides the bias current of the OPD needed to make constant DC bias. The bias current level can be increased to 4.8 μA. After adjusting the DC bias current of OPD, the AC value of the PPG signal is sampled with the 10′b SAR ADC in two successive stages of amplification. In the digital processor, the OLED current is increased until the SNR of the PPG signal exceeds 30 dB. The controllable OLED current range is 60–960 μA with the 4′b control code.

The degradation compensation results are shown below of Fig. 11. The luminance of the green OLED decreases as much as 70% from the original value after 26 days, so that current level of the OLED increases from 180 to 300 μA. After the degradation compensation, the luminance difference is only 2%, which maintains the 30 dB SNR of the PPG signal.

D. Large Parasitic Elements Optimized Design

As mentioned in section II-D, the large parasitic elements of the organic optical sensors can adversely affect the low-power and low-noise operation of the system. In the OLED current driver, a time constant [the product from multiplication of capacitance (C_{OLED}) and resistance (R_{OLED})] limits the frequency response of the OLED. When the 30 dB SNR-guaranteed OLED current level is determined, a duty-cycled control signal is generated from the digital processor. The duty of control signal is varied from 25 to 2%. After the data is sampled with the TIA and SAR ADC, the digital processor chooses whether the frequency response will be

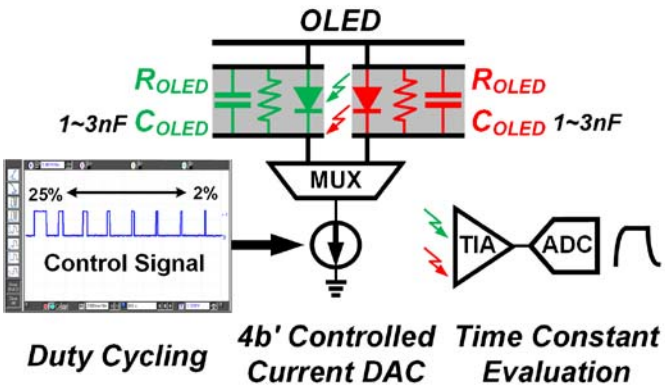

Fig. 12. Large Parasitic Capacitance & Resistance Optimized OLED Driver.

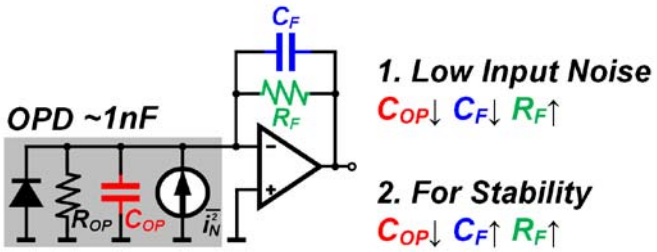

Fig. 13. Large Parasitic Capacitance & Resistance Optimized OPD Sensor Read-out.

limited with the duty of control signal or not, as shown in Fig. 12. The minimum duty cycle is selected for low-power operation.

Because the internal capacitance of the OPD (C_{OP}) is far larger (~1 nF) than a silicon-based photodiode, the feedback capacitor (C_F) and feedback resistor (R_F) should be carefully selected in the OPD sensor read-out circuit. There are two trade-offs for system consideration: input noise and stability, as shown in Fig. 13. The total input-referred noise power spectral density (PSD) of the TIA is given by equation (1) [19].

$$\overline{I_N^2} = 2qI_{IN} + \frac{4kT}{R_F} + \overline{e_{n-op}^2}\left[\frac{1}{R_F^2} + (4\pi f)(C_F + C_{OP})^2\right] \quad (1)$$

Where $\overline{e_{n-op}^2}$ is the input-referred noise voltage power in a CMOS op-amp. The internal capacitance of the OPD directly affects input noise. Larger R_F and lower C_F are required for the low-noise system.

However, another equation is also needed for system stability. When the C_{OP} and R_F are large enough, the requirement of C_F for the stable system is given by equation (2) [23].

$$C_F > \sqrt{\frac{C_{OP}}{GBW \cdot \pi \cdot R_F}} \quad (2)$$

Where GBW is a gain bandwidth of the CMOS op-amp. The minimum value of C_F is determined by equation (2). The values of the optimized elements are required to meet the two conditions at the same time. The O_{PD} value is around 1 nF; so 1 MΩ is selected as R_F for the low-noise system, and 3.1 pF is selected as C_F for the stable system.

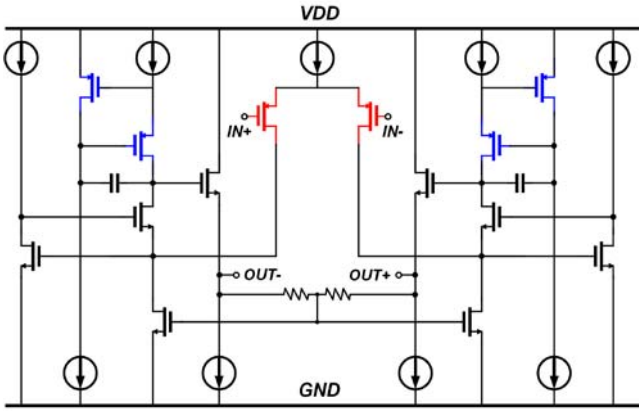

Fig. 14. Schematic of OTA in the Trans-Impedance Amplifier.

The gain boosted OTA is designed with the open-loop voltage gain of 90 dB as shown in Fig. 14. To reduce the 1/f noise, the PMOS MOSFET is adopted for input stage.

E. Motion Artifact Rejection Scheme

As mentioned in section II-E, the motion artifact rejection scheme is a critical requirement of a continuous PPG signal monitoring system. During continuous daily monitoring, a user should have free movement. However, a DC offset can be generated from the user movement; therefore, the measured data could be saturated given the limited supply voltage. The motion artifact rejection scheme (which removes the varying DC offset) is essential for long-term data acquisition.

Contact impedance monitoring is frequently used for motion artifact rejection [24]-[25]. The contact impedance is used as the input data of the least-mean-square (LMS) adaptive filter for DC offset cancellation [24]. Fig. 15 shows the overall architecture of the contact impedance sensor read-out. A 2 kHz frequency of pseudo-sine wave current is generated in the current generator. The current (up to 100μA) is passed through the two electrodes to stimulate the human body. The contact impedance data is measured with the two paths of the amplifier, which has in-phase and quadrature-phase shifts from the current generator. The capacitive feedback low-noise amplifier (LNA) is implemented at the first stage. The input-referred noise of the LNA is 0.57 $\mu V/\sqrt{Hz}$ and the bandwidth is 150 kHz. The total voltage gain can be varied from 4 to 32. The measured contact impedance data is converted with the 10′b SAR ADC and is processed in the internal digital processor.

Fig. 16 shows the pseudo-sine current generator circuit. Two current steering DACs and a bias current generator are implemented for generating a 2-kHz, ~100-μA stimulation current. The 16′b control code for the pseudo-sine wave generation comes from the look-up table (LUT) of the internal digital processor [26]. The 16′b code is enough for suppressing the harmonic components of the stimulation current.

Fig. 17 shows the architecture of the adaptive filter for motion artifact rejection. Two adaptive filters are cascaded implemented for fast settling time [24]. The first stage of the adaptive filter is used to suppress the fluctuation of the DC bias while adjusting the bias current of the OPD.

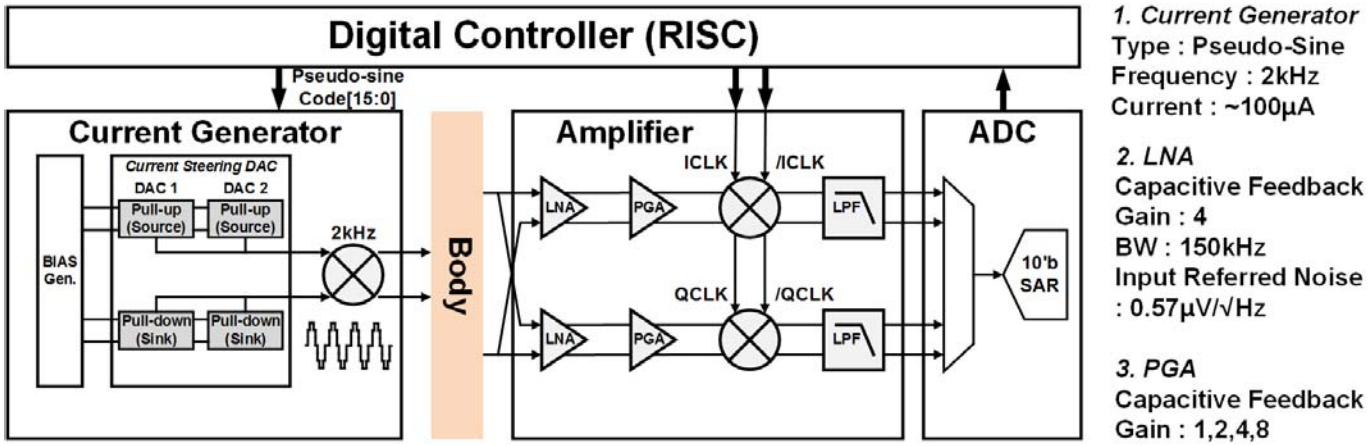

Fig. 15. Overall Architecture of Contact Impedance Sensor Read-out.

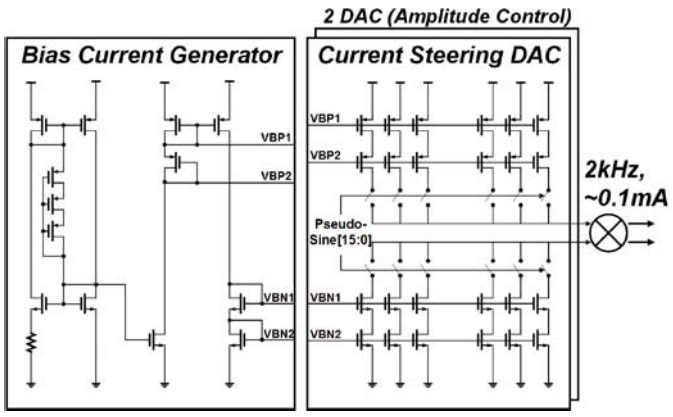

Fig. 16. Pseudo-sine Current Generator Circuit.

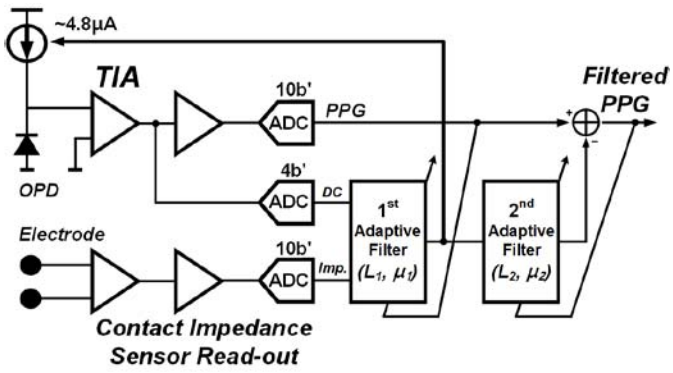

Fig. 17. Adaptive Filter for Motion Artifact Rejection.

The low-frequency components are filtered out in the first stage filter, and the small step-size (μ_1) is adopted because it does not require fast convergence. Not only the contact impedance data, but also the DC component of the measured PPG data is utilized as the input of the first stage adaptive filter. The second stage of the adaptive filter is used to suppress the high-frequency components. The larger step-size (μ_2) has fast convergence time, however the rejection accuracy is reduced. The value of the step-size at the second stage is that it is adaptively settled after several iteration sequences. The proposed motion artifact rejection scheme reduces the

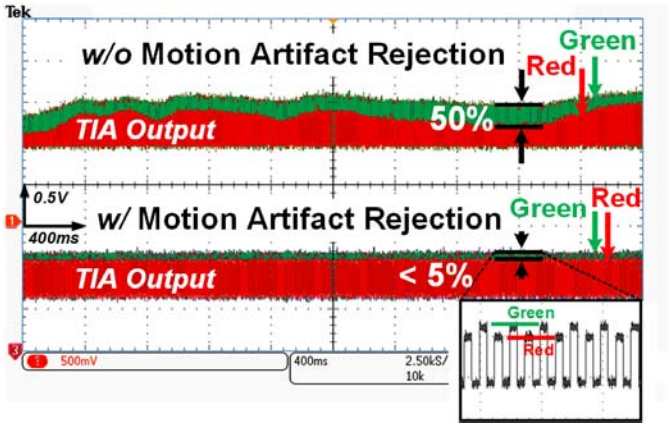

Fig. 18. Motion Artifact Rejection Result.

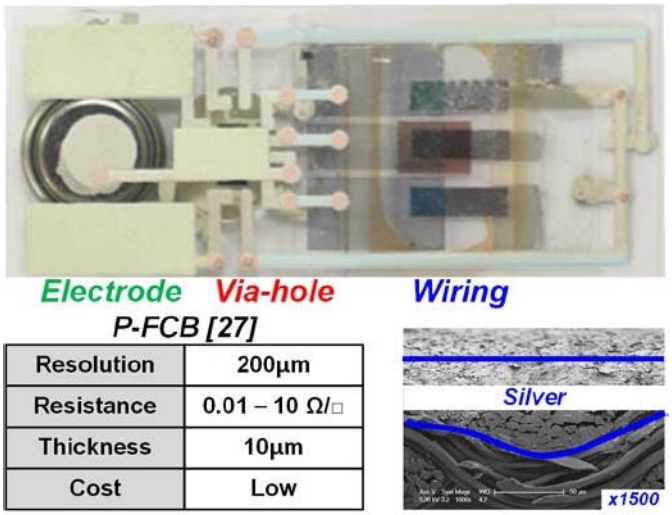

Fig. 19. Specification of the P-FCB Technology.

DC variation from 50 to less than 5 % under the condition of daily movement by the user, as shown in Fig. 18.

IV. P-FCB: Connecting CMOS IC with Organic Sensor

The planar-fashionable circuit board (P-FCB) technology [21] is used for connecting the CMOS IC with the organic

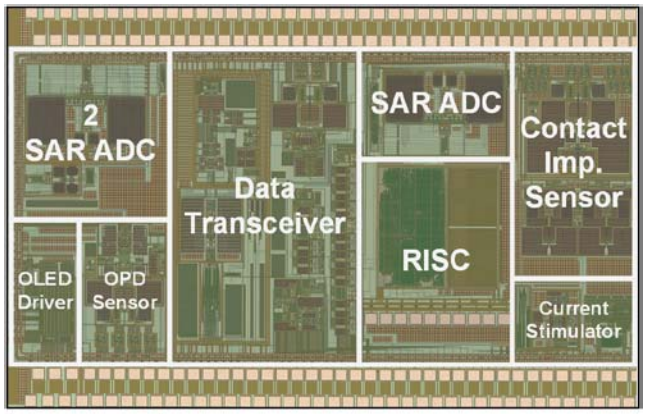

Process		0.18µm 1P6M Mixed CMOS	
Die Size		3.5 X 2.35 mm^2 (Including Pads)	
Main Blocks	OLED Driver	Current Amplitude	60µA ~ 960µA
		Current Duty	2% ~ 25%
	OPD TIA	Gain	1MΩ X 18dB
		Sampling Rate	50Hz ~ 5kHz
	Contact Imp. Sensor	Injected Current	2kHz, ~100µA
		Total Amp. Gain	12dB ~ 30dB
		Input Referred Noise	0.57µV/√Hz
Power		233 µW ~ 1404 µW	

Fig. 20. Chip Micrograph with Performance Summary.

optical sensors. The electrodes, wires, and via-holes can be screen printed with P-FCB technology, as shown in Fig. 19. The measured specifications of the P-FCB silver printing [27] are stated in the table below of Fig. 29. The minimum resolution of P-FCB printing between two wires is 200 μm. The sheet resistance is varied from 0.01 to 10 Ω per square. This minimizes the voltage drop from the wire. The thickness of the P-FCB silver printing is only 10 μm. An enlarged ($\times$1500) SEM micrograph of a cross-section is shown [27]. The screen printed silver is well deposited on the substrate surface.

V. Implementation Results

In this section, implementation results will be discussed. In Fig. 20, the chip photograph and performance summary of the CMOC IC are shown. The proposed CMOS IC is fabricated using a 0.18-μm CMOS process and the area is 8.225 mm^2, including pads. For the PPG signal acquisition, the OLED driver and OPD TIA are implemented in the CMOS IC. Furthermore, the contact impedance sensor with adaptive filter is implemented for motion artifact rejection. The specifications of the three main blocks of the analog front-end are stated in the performance summary. The power consumption, including analog front-end, internal digital processor (RISC), and data transceiver; varies from 233 to 1404 μW.

Fig. 21 shows the PPG signal measurement results from the various body parts (i.e., fingertip, wrist, and neck). Due to the degradation compensation scheme of the CMOS IC, a 30 dB SNR PPG signal is obtained at all times. The ratio of the AC to DC components of the PPG signal differs according

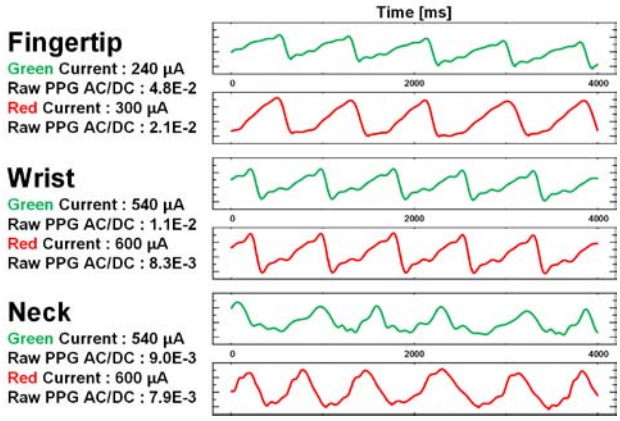

Fig. 21. PPG Signal Measurement Results from Various Body Parts.

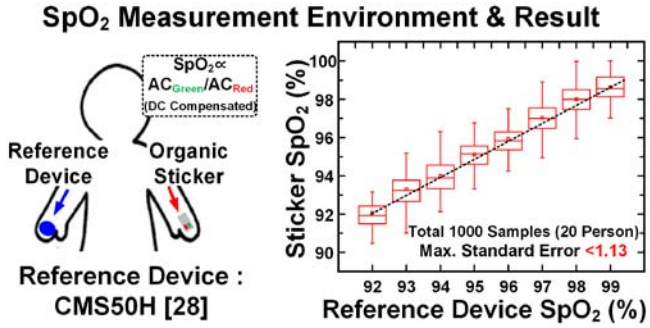

Fig. 22. SpO_2 Measurement Environment and Extraction Result.

TABLE I
Comparison Table

	[5]	[6]	[28]	[29]	This Work
Supply Voltage	9V	5V	N.C.	3V	5V / 1.5V
Power	N.C.	N.C.	N.C.	336 ~ 1545µW	233 ~ 1404µW
LED Duty Cycle	N.C.	N.C.	N.C.	0.7%	2 ~ 25%
LED Driving Current *	~ 30.94mA	~ 9.52mA	~ 40mA	0.1mA ~ 25.6mA	0.06mA ~ 0.96mA
LED/PD Type	Organic (PLED)	Organic (PLED)	Solid-State	Solid-State	Organic (OLED)
Integration Level	Organic Only	Organic Only	Off-the-shelf	CMOS IC Only	CMOS IC + Organic

* Assuming OLED Area : 9.52mm^2 (Same as Proposed Work)

to the body region. In the fingertip, the current level required for the green OLED is 240 μA and the ratio of AC to DC components is higher than 0.04. In the neck, on the contrary, the ratio of AC to DC component is only 0.009; therefore the required current must be two times higher than for the fingertip. Those differences stem from the varying thickness of the epidermis surrounding the blood vessels.

Fig. 22 shows the SpO_2 measurement environment and extraction results. In order to verify the SpO_2 variation with respect to oxygen density, the reference SpO_2 sensor device [28] is located on the right hand and the proposed sticker-type system is attached to the left hand. The SpO_2 value calculated from the measured PPG signal varies from 99 to 93 %. This is very similar to the measured results

from the reference device. Compared with the SpO_2 results from the reference device, the maximum standard error for 1000 samples from 20 people is 1.13 which is only 2% difference.

Table I shows a comparison of results with previously designed PPG signal monitoring systems. Note that proposed system is the first approach with hybrid integration of CMOS IC with the organic optical sensors. The power-efficient low-molecular weight OLED can be operated with one hundredth less current that the previous PLED-based devices. As shown in the table, the proposed system consumes the least power with OLED duty cycling.

VI. Conclusion

In this paper, a method for hybrid integration of a CMOS IC and organic optical sensors is proposed for PPG signal monitoring with a sticker-type system. The P-FCB technology is adopted for connecting the CMOS IC with organic optical sensors. Previously reported devices have several problems for utilization in continuous monitoring. To solve these, five features are provided in the new hybrid system. 1) Power-efficient low-molecular weight based OLEDs are adopted as the light emitting elements. 2) In the CMOS IC, an analog front-end processor and a digital processor are integrated to achieve a small form-factor, low-noise system. 3) The natural degradation of the organic optical sensors is compensated with the CMOS IC. 4) The large parasitic elements of the organic sensors are considered in the analog front-end design. 5) Motion artifact is rejected with the contact impedance sensor and cascaded adaptive filters. The proposed sticker-type PPG monitoring system is hybrid-integrated on the flexible PET substrate, has small area (5.5 $\times$ 2.5 cm), light weight (approx. 2g including batteries) and low-power consumption (233 – 1404 μW). The PPG signal is acquired from various body parts (finger, wrist, and neck), and accurate SpO_2 data is successfully extracted from 20 human subjects. The maximum standard error for 1000 SpO_2 sample results is 1.13, when compares with the measurements done with a commercial reference device.

References

[1] L. G. Lindberg, T. Tamura, and P. A. Oberg, "Photoplethysmography," *Med. Biol. Eng. Comput.*, Jan. 1991.

[2] P. V. Rajesh *et al.*, "A 172μW compressive sampling photoplethysmographic readout with embedded direct heart-rate and variability extraction from compressively sampled data," in *IEEE Int. Solid-State Circuits Conf. (ISSCC) Dig. Tech. Papers*, Feb. 2016, pp. 386–387.

[3] J. E. Sinex, "Pulse oximetry: Principles and limitations," *Amer. J. Emergency Med.*, vol. 17, pp. 59–66, Jan. 1999.

[4] J. Pilling and M. Cutaia, "Ambulatory oximetry monitoring in patients with severe COPD: A preliminary study," *Chest*, vol. 116, no. 2, pp. 314–321, Aug. 1999.

[5] M. Claire, Y. Lochner, Y. Khan, A. Pierr, and A. C. Arias, "All-organic optoelectronic sensor for pulse oximetry," *Nature Commun.*, vol. 5, no. 5745, Dec. 2014.

[6] T. Yokota *et al.*, "Ultra flexible organic photonic skin," *Sci. Adv.*, vol. 2, no. 4, Apr. 2016.

[7] Y. Lee *et al.*, "A 141μW sensor SoC on OLED/OPD substrate for SpO_2/ExG monitoring sticker," in *IEEE Int. Solid-State Circuits Conf. (ISSCC) Dig. Tech. Papers*, Feb. 2016, pp. 384–385.

[8] A. N. Bashkatov, E. A. Genina, V. I. Kochubey, and V. V. Tuchin, "Optical properties of human skin, subcutaneous and mucous tissues in the wavelength range from 400 to 2000nm," *J. Phys. D, Appl. Phys.*, vol. 38, pp. 2543–2555, Jul. 2005.

[9] B. R. Lee *et al.*, "Highly efficient red-emitting hybrid polymer light-emitting diodes via Förster resonance energy transfer based on homogeneous polymer blends with the same polyfluorene backbone," *ACS Appl. Mater. Int.*, vol. 5, pp. 5690–5695, May 2013.

[10] M. Suh *et al.*, "High-efficiency polymer LEDs with fast response times fabricated via selection of electron-injecting conjugated polyelectrolyte backbone structure," *ACS Appl. Mater. Int.*, vol. 7, pp. 26566–26571, Jul. 2015.

[11] Z. Liu, L. Zhang, X. Gao, L. Zhang, Q. Zhang, and J. Chen, "Highly efficient green PLED based on triphenlyaminesilole-carbazole-fluorene copolymers with TPBI as the hole blocking layer," *Dyes Pigments*, vol. 127, pp. 155–160, Dec. 2015.

[12] G. Cheng, P.-K. Chow, S. C. F. Kui, C.-C. Kwok, and C.-M. Che, "High-efficiency polymer light-emitting devices with robust phosphorescent platinum(II) emitters containing tetradentate dianionic O^N^C^N ligands," *Adv. Mater*, vol. 25, pp. 6765–6770, Aug. 2013.

[13] J. Xu *et al.*, "A wearable 8-channel active-electrode EEG/ETI acquisition system for body area networks," *IEEE J. Solid-State Circuits*, vol. 49, no. 9, pp. 2005–2016, Sep. 2014.

[14] J. Xu, B. Büsze, C. Van Hoof, K. A. A. Makinwa, and R. F. Yazicioglu, "A 15-channel digital active electrode system for multi-parameter biopotential measurement," *IEEE J. Solid-State Circuits*, vol. 50, no. 9, pp. 2090–2100, Sep. 2015.

[15] G. R. Chaji *et al.*, "Electrical compensation of OLED luminance degradation," *IEEE Electron Device Lett.*, vol. 28, no. 12, pp. 1108–1110, Dec. 2007.

[16] M. Schaer, F. Nüesch, D. Berner, W. Leo, and L. Zuppiroli, "Water vapor and oxygen degradation mechanisms in organic light emitting diodes," *Adv. Mater*, vol. 11, no. 2, pp. 116–121, Apr. 2001.

[17] S. Hong *et al.*, "Technologies for flexible AMOLEDs," *Inf. Display*, vol. 31, no. 1, pp. 6–11, 2015.

[18] S.-S. Lee, "Parameter analysis of an organic light-emitting diode (OLED)," *J. Korean Phys. Soc.*, vol. 53, no. 2, pp. 840–844, Aug. 2008.

[19] M. Crescentini, M. Bennati, M. Carminati, and M. Tartagni, "Noise limits of CMOS current interfaces for biosensors: A review," *IEEE Trans. Biomed. Circuits Syst.*, vol. 8, no. 2, pp. 278–292, Apr. 2014.

[20] J. Yao and S. Warren, "A short study to assess the potential of independent component analysis for motion artifact separation in wearable pulse oximeter signals," in *Proc. IEEE Eng. Med. Biol. 27th Annu. Conf.*, Aug. 2005, pp. 3585–3588.

[21] H. Kim, Y. Kim, Y.-S. Kwon, and H.-J. Yoo, "A 1.12 mW continuous healthcare monitor chip integrated on a planar-fashionable circuit board," in *IEEE Int. Solid-State Circuits Conf. (ISSCC) Dig. Tech. Papers*, Feb. 2008, pp. 150–151.

[22] M. Zhang, H. Wang, H. Tian, Y. Geng, and C. W. Tang, "Bulk heterojunction photovoltaic cells with low donor concentration," *Adv. Mater.*, vol. 42, no. 24, pp. 4960–4964, Dec. 2011.

[23] Linear Technology Inc. *Product Specification for LTC6268/LTC6269*. [Online]. Available: http://cds.linear.com/docs/en/datasheet/62689f.pdf

[24] H. Kim *et al.*, "Motion artifact removal using cascade adaptive filtering for ambulatory ECG monitoring system," in *Proc. IEEE Biomed. Circuits Syst. Conf. (BioCAS)*, Nov. 2012, pp. 160–163.

[25] N. V. Helleputte *et al.*, "A 345 μW multi-sensor biomedical SoC with bio-impedance, 3-channel ECG, motion artifact reduction, and integrated DSP," *IEEE J. Solid-State Circuits*, vol. 50, no. 1, pp. 230–244, Jan. 2015.

[26] Y. Lee, K. Song, and H.-J. Yoo, "A 4.84mW 30fps dual frequency division multiplexing electrical impedance tomography SoC for lung ventilation monitoring system," in *Proc. Symp. VLSI Circuits (VLSI Circuits)*, Jun. 2015, pp. C204–C205.

[27] J. Yoo, L. Yan, S. Lee, H. Kim, and H.-J. Yoo, "A wearable ECG acquisition system with compact planar-fashionable circuit board-based shirt," *IEEE Trans. Inf. Technol. Biomed.*, vol. 13, no. 6, pp. 897–902, Nov. 2009.

[28] *CMS50H*, Contec Med. Syst. Co., 2011.

[29] E. S. Winokur, T. O'Dwyer, and C. G. Sodini, "A low-power, dual-wavelength photoplethysmogram (PPG) SoC with static and time-varying interferer removal," *IEEE Trans. Biomed. Circuits Syst.*, vol. 9, no. 4, pp. 581–589, Aug. 2015.

Yongsu Lee (S'13) received the B.S. and M.S. degree in electrical engineering from Korea Advanced Institute of Science and Technology (KAIST), Daejeon, Korea, in 2013 and 2015, where he is currently working toward the Ph.D. degree.

His current research interests include low-power bio-medical SoC for wearable healthcare systems. He is also interested in human body communication (HBC) SoC for low-power applications.

Hyeonwoo Lee (S'14) received the B.S. and M.S. degree in electrical engineering from Korea Advanced Institute of Science and Technology (KAIST), Daejeon, Korea, in 2014 and 2016, where he is currently working toward the Ph.D. degree.

His current research focuses on organic electronics for wearable healthcare application.

Jaeeun Jang (S'13) received B.S. degree in electrical engineering from the Korea

Advanced Institute of Science and Technology (KAIST), Daejeon, Korea, in 2014, where he is currently working toward the M.S. degree. He has worked on developing a low-power wireless transceiver and low-power sensor front-end. His current research interest includes low power transceiver design for body-area-networks and low-power bio-medical SoC design.

Jihee Lee (S'15) received the B.S. degree in electrical engineering from Korea Advanced Institute of Science and Technology (KAIST), Daejeon, Korea, in 2015 where she is currently working toward the M.S. degree.

Her current research interests include low-power bio-medical SoC for wearable healthcare system. She is also interested in energy harvesting and human body communication (HBC) SoC for low-power application.

Minseo Kim (S'14) received the B.S degree in Semiconductor System Engineering, Sung Kyun Kwan University in 2014 and received M.S. degree in electrical engineering from Korea Advanced Institute of Science and Technology (KAIST), Daejeon, Korea, in 2016, where he is currently working toward the Ph.D. degree.

His current research interests include low-power bio-medical SoC for wearable healthcare system.

Jaehyuk Lee (S'12) received the B.S. degree in electrical engineering from the Korea Advanced Institute of Science and Technology (KAIST), Daejeon, Korea, in 2014, where he is currently working toward the M.S. degree. His current research interests include biomedical system design and verification, especially focused on electrical stimulator and biosignal sensor. He is also interested in body-channel communication for low-power wireless body area network (WBAN).

Hyunki Kim (S'13) received the B.S. degree in mathematical sciences and the M.S. degree in Electrical Engineering from the Korea Advanced Institute of Science and Technology (KAIST), Daejeon, Korea, in 2010 and 2015, respectively.

Currently, he is working toward the Ph.D. degree at KAIST. His research interests include biomedical SoC design, especially focused on low-power signal processors.

Seunghyup Yoo (M'08) received his B.S. and M.S. degrees in Physics from Seoul National University, Seoul, Korea, in 1996 and 1998, respectively, and the Ph.D. degree in Optical Sciences from the University of Arizona, Tucson, in 2005 for his work on organic thin-film solar cells based on pentacene/C60 heterojunctions. From 2005 to 2006, he was a post-doctoral researcher at the School of Electrical and Computer Engineering, Georgia Institute of Technology, Atlanta, where he worked on various organic optoelectronic devices. Since August 2006, he has been with the Faculty of the School of Electrical Engineering, Korea Advanced Institute of Science and Technology, Daejeon, Korea, where he is currently a full Professor. His major research interests include the development of a novel device architecture and process for organic/printed electronics in the areas of display/lighting, energy, and low-cost electronics.

Hoi-Jun Yoo (M'95–SM'04–F'08) graduated from the Electronic Department of Seoul National University, Seoul, Korea, in 1983 and received the M.S. and Ph.D. degrees in electrical engineering from the Korea Advanced Institute of Science and Technology (KAIST), Daejeon, in 1985 and 1988, respectively.

Since 1998, he has been the faculty of the Department of Electrical Engineering at KAIST and now is a full professor. From 2001 to 2005, he was the director of Korean System Integration and IP Authoring Research Center (SIPAC). From 2003 to 2005, he was the full time Advisor to Minister of Korea Ministry of Information and Communication and National Project Manager for SoC and Computer. In 2007, he founded System Design Innovation & Application Research Center (SDIA) at KAIST. Since 2010, he has served the general chair of Korean Institute of Next Generation Computing. His current interests are computer vision SoC, body area networks, biomedical devices and circuits. He is a co-author of DRAM Design (Korea: Hongrung, 1996), High Performance DRAM (Korea: Sigma, 1999), Future Memory: FRAM (Korea: Sigma, 2000), Networks on Chips (Morgan Kaufmann, 2006), Low-Power NoC for High-Performance SoC Design (CRC Press, 2008), Circuits at the Nanoscale (CRC Press, 2009), Embedded Memories for Nano-Scale VLSIs (Springer, 2009), Mobile 3D Graphics SoC from Algorithm to Chip (Wiley, 2010), Bio-Medical CMOS ICs (Springer, 2011), Embedded Systems (Wiley, 2012), and Ultra-Low-Power Short-Range Radios (Springer, 2015).

Dr. Yoo received the Electronic Industrial Association of Korea Award for his contribution to DRAM technology in 1994, Hynix Development Award in 1995, the Korea Semiconductor Industry Association Award in 2002, Best Research of KAIST Award in 2007, Scientist/Engineer of this month Award from Ministry of Education, Science and Technology of Korea in 2010, Best Scholarship Awards of KAIST in 2011, and Order of Service Merit from Ministry of Public Administration and Security of Korea in 2011 and has been co-recipients of ASP-DAC Design Award 2001, Outstanding Design Awards of 2005, 2006, 2007, 2010, 2011, 2014 A-SSCC, Student Design Contest Award of 2007, 2008, 2010, 2011 DAC/ISSCC. He has served as a member of the executive committee of ISSCC, Symposium on VLSI, and A-SSCC and the TPC chair of the A-SSCC 2008 and ISWC 2010, IEEE Fellow, IEEE Distinguished Lecturer ('10-'11), Far East Chair of ISSCC ('11-'12), Technology Direction Sub-Committee Chair of ISSCC ('13), TPC Vice Chair of ISSCC ('14), and TPC Chair of ISSCC ('15).